Sensitivity studies for the main r process: nuclear masses

A. Aprahamian, I. Bentley, M. Mumpower, and R. Surman

Citation: AIP Advances **4**, 041101 (2014); doi: 10.1063/1.4867193
View online: http://dx.doi.org/10.1063/1.4867193
View Table of Contents: http://scitation.aip.org/content/aip/journal/adva/4/4?ver=pdfcov
Published by the AIP Publishing

AIP ADVANCES **4**, 041101 (2014)

Sensitivity studies for the main *r* process: nuclear masses

A. Aprahamian,[1] I. Bentley,[2] M. Mumpower,[1] and R. Surman[3]
[1]*Department of Physics, University of Notre Dame, Notre Dame, IN 46556 USA*
[2]*Department of Chemistry and Physics, St. Mary's College, Notre Dame, IN 46556 USA*
[3]*Department of Physics and Astronomy, Union College, Schenectady, NY 12308 USA*

(Received 12 December 2013; accepted 13 February 2014; published online 26 February 2014)

The site of the rapid neutron capture process (*r* process) is one of the open challenges in all of physics today. The *r* process is thought to be responsible for the creation of more than half of all elements beyond iron. The scientific challenges to understanding the origin of the heavy elements beyond iron lie in both the uncertainties associated with astrophysical conditions that are needed to allow an *r* process to occur and a vast lack of knowledge about the properties of nuclei far from stability. One way is to disentangle the nuclear and astrophysical components of the question. On the nuclear physics side, there is great global competition to access and measure the most exotic nuclei that existing facilities can reach, while simultaneously building new, more powerful accelerators to make even more exotic nuclei. On the astrophysics side, various astrophysical scenarios for the production of the heaviest elements have been proposed but open questions remain. This paper reports on a sensitivity study of the *r* process to determine the most crucial nuclear masses to measure using an *r*-process simulation code, several mass models (FRDM, Duflo-Zuker, and HFB-21), and three potential astrophysical scenarios. © *2014 Author(s). All article content, except where otherwise noted, is licensed under a Creative Commons Attribution 3.0 Unported License.* [http://dx.doi.org/10.1063/1.4867193]

I. INTRODUCTION

The origins of nuclei beyond iron are entangled in complexity since the heavier elements are thought to be made via both slow- and rapid- neutron-capture processes (*s* and *r* processes).[1] The *s* process leads to a network of nuclei near stability while the *r* process allows the production of nuclei with increasing neutron numbers much further from stability, producing neutron-rich nuclei. The astrophysical scenarios in which the *s* process can take place have been identified but a potential site for the *r* process is still unresolved.[2,3] The challenge for astrophysical science today is to understand the conditions that would provide a major abundance of neutrons and lead to sufficient successive captures and decays to build up the heaviest elements, while on the nuclear side, the challenge is to determine the physics of nuclei far from stability where the range and impact of the nuclear force is less well known.[2,4] There have been a number of astrophysical scenarios suggested as possible sites for the *r* process but each of them has its own drawbacks. Some of the most promising potential sites include the neutrino driven wind from core-collapse supernovae,[5–8] two-neutron star mergers,[9–11] gamma ray bursts,[12,13] black-hole neutron star mergers,[14] and relativistic or magnetohydrodynamic jets from supernovae.[15–17]

On the nuclear physics side, the challenge lies in the ability of nuclear models to predict properties of nuclei far from stability where measurements are difficult or not possible. Fig. 1 shows the mass excess values normalized to the theoretical finite range droplet model (FRDM)[18] values for a series of cadmium isotopes as a function of neutron number. The black boxes are the measured values whereas the open boxes are those extrapolated in the latest evaluation of masses (AME2012).[19] The agreement of experiment and theory is remarkably good in the measured region

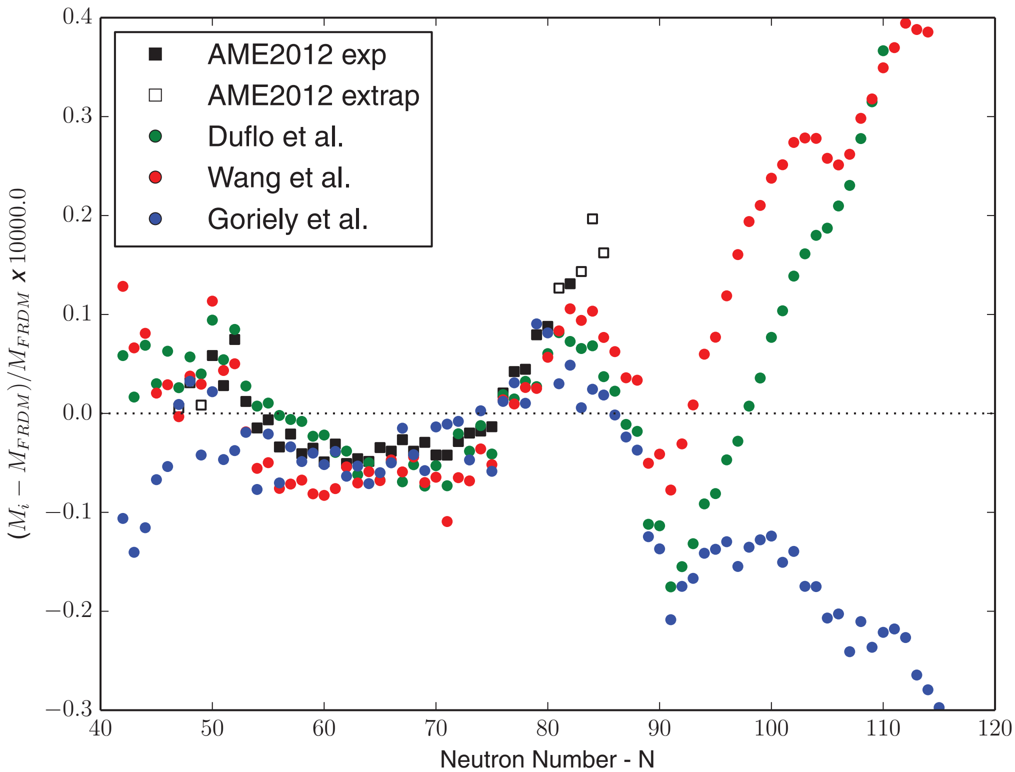

FIG. 1. The mass excess of cadmium isotopes consisting of experimental (filled boxes) and extrapolated (open boxes) values from AME2012[19] compared to theoretical values from Duflo & Zuker,[20] Goriely *et al.*,[21] and Wang *et al.*,[22] expressed as fractional differences from the FRDM values.[18]

but diverges farther from stability, and in some cases the divergences are themselves in opposite directions.

On the experimental side of nuclear physics, the study of radioactive nuclei far from stability approaching a possible *r*-process path is one of the global research frontiers for nuclear science today. New facilities are being developed in the USA (CARIBU at ANL, NSCL and FRIB at MSU), in Europe (ISOLDE at CERN), in France (SPIRAL II at GANIL), in Finland (Jyvaskyla), in Germany (FAIR at GSI Darmstadt), in Japan (RIKEN), in China (BRIF,CARIF in CIAE Beijing), and in Canada (ISAC at TRIUMF).

An important overarching question for this global effort in nuclear science is which measurements need to be made in order remove or diminish some of the uncertainties associated with the nuclear properties[23] input into simulations of the *r* process. The *r* process proceeds via a sequence of neutron captures, photodissociations, and β decays. Simulations of the *r* process therefore require tabulations of neutron capture rates, β-decay half-lives, and neutron separation energies for thousands of nuclei far from stability. The latter are used to calculate the photodissociation rates $\lambda_\gamma(Z, A)$ by detailed balance:

$$\lambda_\gamma(Z, A) \propto T^{3/2} \exp\left[-\frac{S_n(Z, A)}{kT}\right] \langle\sigma v\rangle_{(Z,A-1)}, \tag{1}$$

where T is the temperature, $S_n(Z, A)$ is the neutron separation energy, and $\langle\sigma v\rangle_{(Z,A-1)}$ is the thermally-averaged value of the neutron capture cross section for the neighboring nucleus with one less neutron. Only a handful of the required pieces of nuclear data have been determined experimentally, and predictions from different theoretical approaches disagree markedly far from stability, e.g. Fig. 1.

II. SENSITIVITY STUDIES: SEPARATION ENERGIES AND NUCLEAR BINDING ENERGIES

As a first step, we focused on the sensitivity of the *r*-process to *individual* neutron separation energies, as they appear in Eq. (1), in an attempt to determine the nuclei that have the greatest impact on the overall *r*-process abundances and in turn to identify the most crucial measurements to be made. The results of this first study appear in Brett *et al.*[24] This was the first time that such a comprehensive attempt was made and the results have been of great interest to the experimental nuclear science community in planning day-one experiments at the various new facilities allowing access to measurements of exotic nuclei.

Neutron separation energies appear explicitly in the calculation of photo-dissociation rates as shown in Eq. (1). In Brett *et al.*,[24] the neutron separation energies were individually varied from their theoretical values by ±25%. Thus this first effort was in effect a photo-dissociation rate sensitivity study, as each separation energy depends on two nuclear masses. In addition, nuclear masses are important components in the calculation of other pieces of nuclear data used in the *r*-process network calculation. Therefore in order to obtain the full measure of the impact of an individual mass on the *r* process, a variation in a single nuclear mass should be propagated to all of the neutron separation energies, neutron capture rates, β-decay rates, and β-delayed neutron emission probabilities that depend on that mass. A fully consistent mass sensitivity study of this type is our ultimate goal and is in progress.[25]

As an intermediate step, here we report on sensitivity studies that go one level deeper from Brett *et al.* and looked into the effects of varying individual nuclear masses, instead of individual separation energies, on the resulting photodissociation rates. The general approach to the sensitivity studies remained the same, except here individual nuclear mass variations for each nucleus (Z, A) were propagated through to the neutron separation energies of (Z, A) and (Z, $A+1$) that depend on that mass.

We started with the astrophysical conditions used in Brett *et al.* based on the 'H' or high frequency *r* process suggested by Qian,[26] with an initial temperature of $T_9 = 1.5$ and an initial density of 3.4×10^2 g/cm^3. We took the temperature and density to decline exponentially as in Ref. 27 with a dynamical timescale of 0.86 s. While Qian specifies a seed of ^{90}Se and a neutron to seed ratio (N_n/N_{seed}) of 86,[26] a lighter seed of ^{70}Fe was chosen, which results in $N_n/N_{seed} = 67$ when the electron fraction is kept consistent with Qian ($Y_e = 0.190$). For the *r*-process simulations we used the nuclear network code from Ref. 28. It is an *r*-process network code that includes neutron captures, photo-dissociations, β decay, and β-delayed neutron emission rates. The network also has the possibilities for the inclusion of fission recycling and neutrino-nucleus interactions, but these options were not used for the sensitivity studies reported here. The measured nuclear masses in this simulation were obtained from the AME2003 compilation of masses. For those nuclei where no measurements were available, we use nuclear masses from the FRDM,[18] DZ (Duflo-Zuker),[20] or HFB-21.[21] Neutron capture rates are from Rauscher[29] or calculated with TALYS[30] to be consistent with the mass models. The beta decay rates are from the FRDM.[31]

We chose the size of the mass variation for the binding energy sensitivity studies by comparing several theoretical mass models far from stability. Since disagreements between the various models can often exceed by one to several MeV, we chose ±1 MeV for the mass variations. Then we individually varied the nuclear masses of each nucleus (Z_{BE}, A_{BE}) in the network in turn, reran the simulation, and compared the results to the baseline. Example abundance patterns resulting from this procedure are compared to the baseline pattern in Fig. 2. The final mass fractions of the simulations $X(A)$ were then compared to those of the baseline simulation $X_{\mathrm{baseline}}(A)$ using a global sensitivity measure $F(Z_{BE}, A_{BE})$:

$$F(Z_{BE}, A_{BE}) = 100 \times \sum_A |X_{\mathrm{baseline}}(A) - X(A)|. \tag{2}$$

The mass fractions are themselves related to the abundances $Y(A)$ by $X(A) = AY(A)$, and $\sum_A X(A) = 1$. This process is repeated for every nuclear mass, resulting in a sensitivity measure $F(Z_{BE}, A_{BE})$ determined for each nucleus in the network.

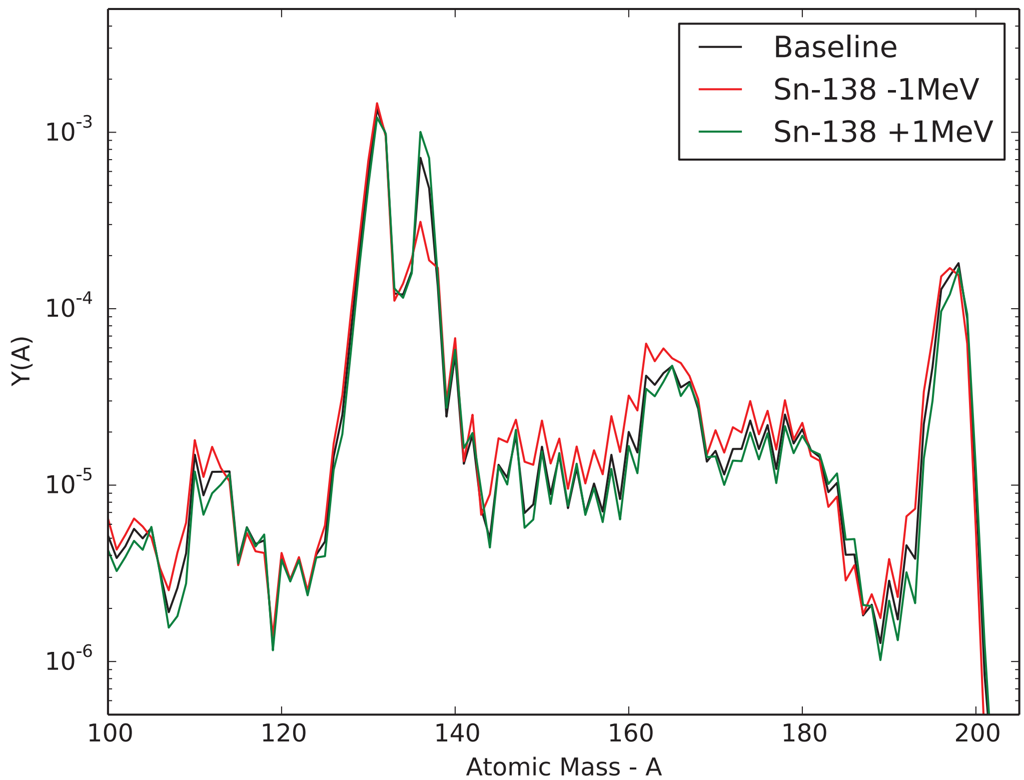

FIG. 2. The final abundances $Y(A)$ versus mass number A for the baseline trajectory (black line) used here and in Brett *et al.*,[24] similar to the 'H' trajectory from Qian.[26] The simulation is repeated for increases (green line) and decreases (red line) in the binding energy of ^{138}Sn of 1 MeV. Note a change in this one mass modifies the final abundance pattern both locally and globally.

III. RESULTS AND DISCUSSION

The results of the binding energy sensitivity study for the three sets of nuclear masses chosen above are presented in Fig. 3. This figure shows the same bulk features as the separation energy sensitivity studies shown in Fig. 3 of Brett *et al.*[24] That is, the largest concentration of nuclei with great impact on the *r*-process as determined from the binding energy sensitivity studies and the separation energy sensitivity studies are along and near the equilibrium *r*-process path, particularly around the closed shells. While (n, γ)-(γ, n) equilibrium persists, the masses determine the abundances along an isotopic chain. Thus a change to a single mass can shift how the *r*-process path is populated. This shift can have global consequences to the *r*-process pattern if it is to an isotope with a markedly faster or slower β-decay lifetime, which can alter the rates at which neutrons are consumed and material moves to higher A. Fig. 4 of Brett *et al.*[24] shows this effect. It can be produced by either a change to a binding energy or a separation energy, thus an exact overlap is expected and observed for the most sensitive nuclei identified by the binding energy and the separation energy studies.

The binding energy and the separation energy studies do show some differences, however, in the results for nuclei closer to stability. These nuclei are populated in later times in the *r* process, during freezeout from (n, γ)-(γ, n) equilibrium, when neutron captures, photodissociations, and β decays all compete and the *r*-process abundance pattern is finalized. A change to an individual neutron separation energy will produce a change in the corresponding photodissociation rate (Eq. (1)), which can alter the post-equilibrium nuclear flow.[35] The potential impact is greatest for odd-N nuclei, because these nuclei fall out of equilibrium much earlier than even-N nuclei, when the conditions are more likely to be sufficiently hot for photodissociation rates to be important. This can be seen in the strong odd-even staggering of sensitivities for nuclei closer to stability in Fig. 3 of Brett *et al.*[24] The odd-even difference is washed out in Fig. 3, because in the binding energy sensitivity

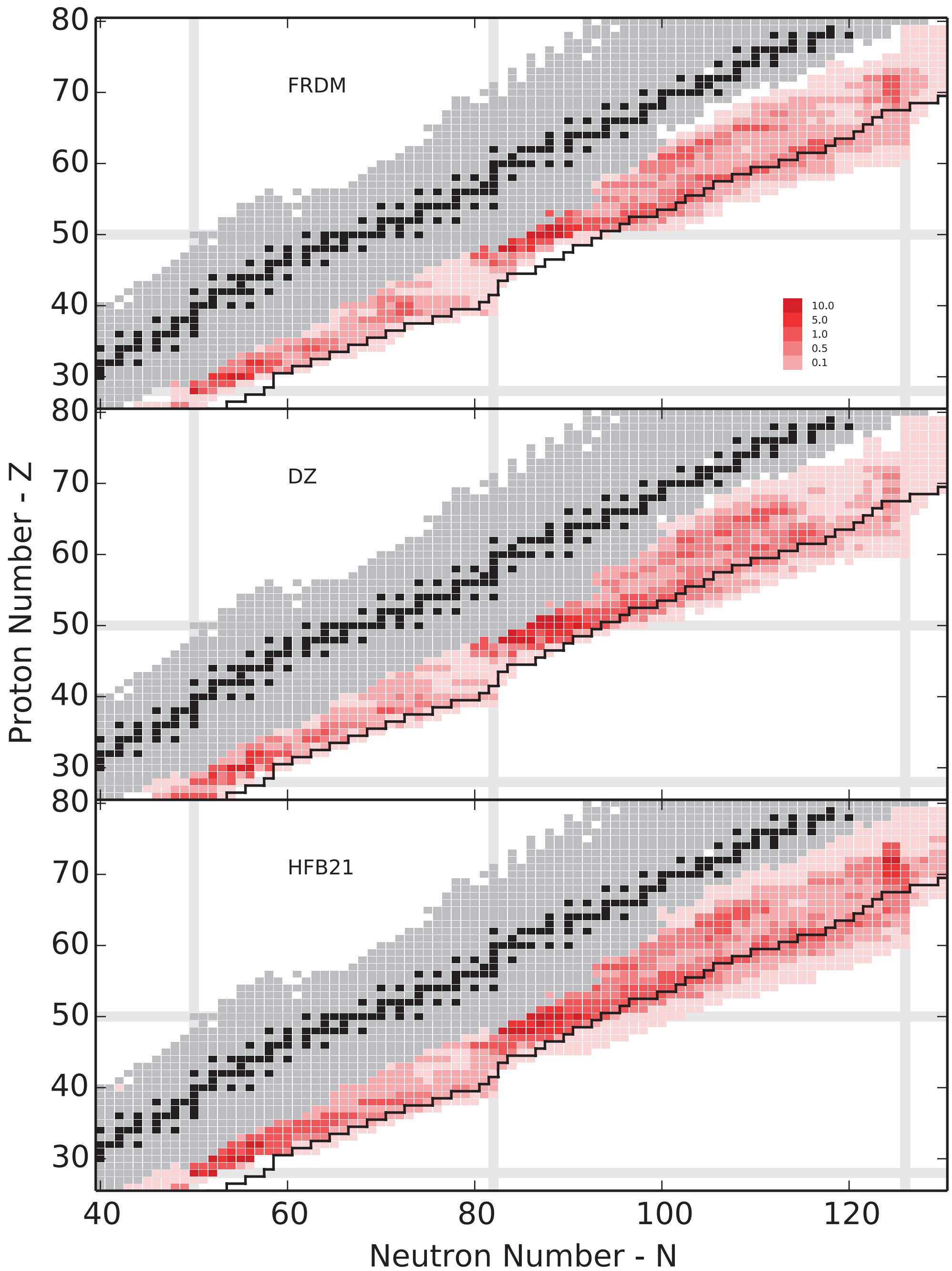

FIG. 3. Sensitivity measures $F(Z_{BE}, A_{BE})$ for each nucleus in the network, for three binding energy sensitivity studies using FRDM[18] (top panel), DZ[20] (middle panel), and HFB-21[21] (bottom panel) masses. All three studies use binding energy variations of ± 1 MeV and astrophysical conditions as used in Brett *et al.*,[24] similar to the 'H' trajectory from Qian.[26] Stable nuclei are represented by solid black boxes. Overlaid in gray is the region of nuclear masses that have been reported as measured in AME2012[19] and the solid black line represents the predicted limits of accessibility for the production rates from FRIB.[32] It is clear from the concentration of F intensities that FRIB will allow the measurements of a significant portion of the most impactful nuclei.

study a variation in the odd-N separation energy is produced by either the alteration of the binding energy of that nucleus or its adjacent even-N neighbor. Thus while Fig. 3 of Brett *et al.*[24] highlights an interesting feature of late-time r-process dynamics, Fig. 3 of this work is a better representation of the impact of individual masses on the r-process pattern.

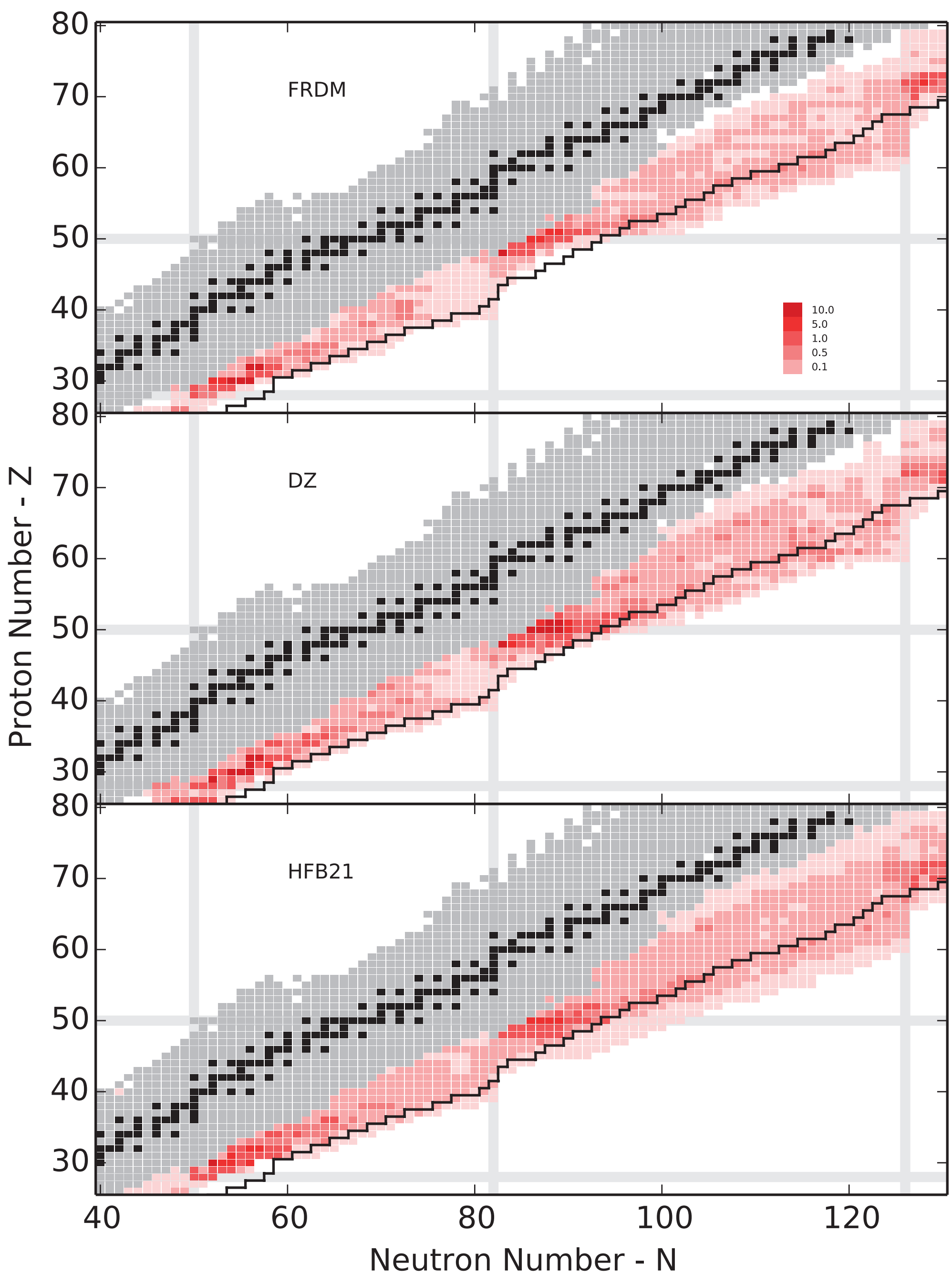

FIG. 4. Results from the three binding energy sensitivity studies shown in Fig. 3, expressed here in terms of an alternate sensitivity measure, $f(Z_{BE}, A_{BE}) = 100 \times \sum_A |Y_{\rm baseline}(A) - Y(A)|/Y_{\rm baseline}(A)$, which emphasizes fractional abundance changes. This sensitivity measure is a sum of percentages, so it is scaled down by a factor of 1000 for the figure. The general features of the binding energy sensitivities are the same regardless of the measure used to quantify them.

There are also some minor differences between the three mass models shown in Fig. 3 for the binding energy sensitivity studies. However, there is a significant overlap in the nuclei that rise to the surface. This overlap, as well as the same general features of the sensitivities, persist even when an alternate measure of sensitivity is used, as shown in Fig. 4. Table I lists the nuclei with a sensitivity measure $F(Z_{BE}, A_{BE})$ greater than 6 in each of the three models. This table was the basis of a recent proposal to CARIBU at ANL to measure nuclear masses. The proposal was given a priority I ranking

TABLE I. The nuclei with the greatest sensitivity measures F ($F > 6$) from Fig. 3.

FRDM				DZ				HFB21			
Z	A	N	F	Z	A	N	F	Z	A	N	F
48	131	83	47.92	50	135	85	40.18	48	131	83	28.76
48	130	82	34.49	48	130	82	36.81	50	137	87	28.52
50	137	87	33.36	50	134	84	35.09	50	136	86	28.32
50	134	84	28.34	50	138	88	34.45	50	139	89	27.18
50	135	85	27.25	50	137	87	32.95	50	138	88	26.20
50	136	86	24.00	50	136	86	31.55	48	130	82	26.06
51	140	89	19.98	48	132	84	29.96	48	132	84	19.93
50	138	88	19.37	48	131	83	28.14	48	133	85	18.97
51	139	88	17.18	48	134	86	26.73	30	84	54	14.90
28	78	50	16.27	50	133	83	24.54	28	78	50	14.48
48	132	84	15.59	50	139	89	23.46	30	82	52	13.69
50	133	83	12.63	50	132	82	22.46	28	80	52	13.20
30	84	54	11.94	30	84	54	21.43	30	86	56	11.67
50	132	82	11.74	51	140	89	20.05	50	141	91	11.43
30	85	55	11.61	30	86	56	19.16	72	196	124	11.03
49	131	82	11.42	51	139	88	18.08	72	197	125	11.03
50	139	89	11.11	30	85	55	17.14	32	89	57	10.90
49	132	83	11.01	48	133	85	16.15	30	85	55	10.86
30	86	56	9.768	51	138	87	15.97	49	136	87	10.77
51	137	86	9.444	51	134	83	15.12	48	134	86	10.47
50	140	90	8.913	51	137	86	14.98	32	88	56	10.08
32	89	57	8.612	49	133	84	14.26	50	140	90	9.975
32	88	56	8.596	49	131	82	13.05	30	83	53	9.798
48	134	86	8.369	51	135	84	12.23	28	79	51	9.515
51	141	90	7.778	51	136	85	11.74	48	137	89	8.865
51	136	85	7.757	50	141	91	10.31	49	133	84	8.336
51	142	91	7.111	32	88	56	9.988	31	85	54	8.316
49	133	84	6.678	32	89	57	9.542	71	196	125	8.054
30	83	53	6.227	48	136	88	9.408	49	135	86	7.868
				49	137	88	8.914	49	131	82	7.600
				49	132	83	8.743	71	195	124	7.336
				49	135	86	8.404	49	132	83	7.328
				51	141	90	8.240	48	136	88	7.259
				50	142	92	8.180	49	137	88	6.809
				51	142	91	8.136	49	138	89	6.539
				51	133	82	7.817	31	87	56	6.531
				49	139	90	7.177	49	134	85	6.271
				49	134	85	6.934	50	134	84	6.106
				29	81	52	6.934				
				31	87	56	6.791				
				50	140	90	6.579				

and 30 days of beam time and will result in a number of measurements of nuclei of great impact to the *r* process.

In brief, this binding energy sensitivity study involving three mass models and one astrophysical trajectory highlights the similarities and differences between the various mass models. Fig. 1 shows the divergences of the various mass models, sometimes in opposite directions, particularly in regions where there are no existing measurements. An important correlated question is the impact of the astrophysical conditions on the *r*-process path and therefore on the nuclei of greatest impact on the abundances resulting from them. The temperature and neutron number density determine the path and therefore the nuclei that lie along the path. Figs. 2 and 3 and Table I are the results from one fixed 'hot' *r*-process trajectory.

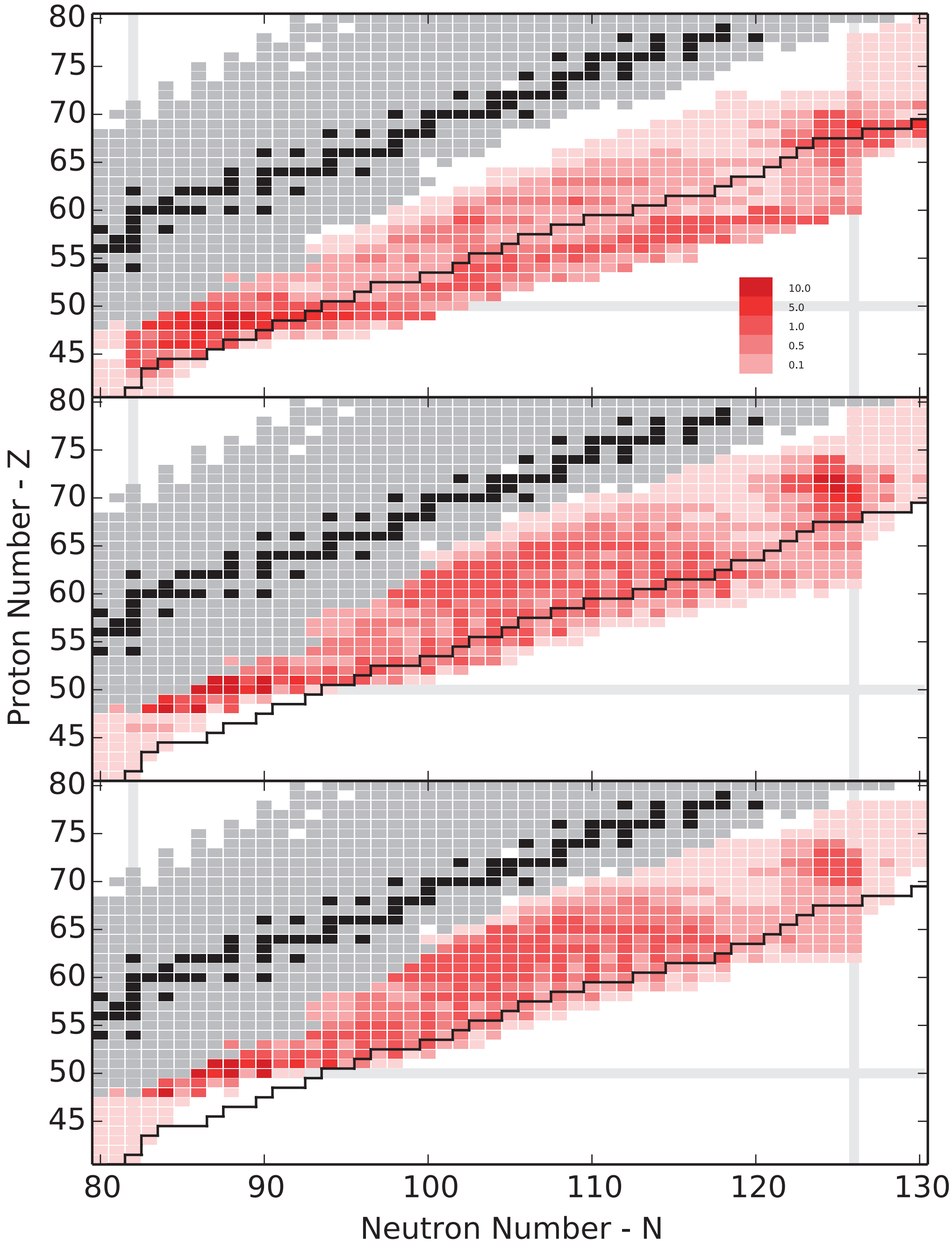

FIG. 5. The sensitivities measures $F(Z_{BE}, A_{BE})$ resulting from three sensitivity studies where binding energies of individual nuclei (Z_{BE}, A_{BE}) were varied by ± 1MeV. The three sensitivity studies start with three distinct sets of astrophysical conditions, as described in the text, with entropy per baryon of $s/k = 10$ (top panel), 100 (middle panel), and 200 (bottom panel). The gray boxes, similar to Fig. 2, show the extent of measurements reported in the AME2012 compilation while the black line is the predicted FRIB production.

In order to explore the effects of the astrophysical scenarios on the binding energy sensitivity studies, we repeated our studies using alternate baseline simulations resulting from three different astrophysical trajectories but the same mass model (FRDM[18]). The astrophysical conditions determine the location of the the *r*-process path, which is set by the temperature and neutron number density. Therefore, repeating the sensitivity study with different temperature and density conditions should shift the *r*-process path and along with it, the nuclei with the highest sensitivity measures F. Different astrophysical conditions will also influence how the material along the *r*-process path in equilibrium moves toward stability at late times. During these late times, individual photodissociation rates can influence the availability of free neutrons via the photodissociation effect identified in Ref. 35. The range of nuclei for which this effect produces significantly noticeable changes with regards to the final abundance patterns is strongly tied to the late-time evolution of the temperature and density.[36]

Fig. 5 graphically shows the evolution of the most impactful nuclei as a function of the three astrophysical trajectories using the same mass model (FRDM[18]) for all three. The trajectories are based on the adiabatic wind parameterization of Meyer[33] as implemented in Mumpower *et al.*,[34] with dynamic timescale $\tau_{\rm dyn} = 80$ ms and three choices of entropy per baryon, $s/k = 10$, 100, and 200. For each set of conditions, the initial composition at $T = 10$ GK is chosen to produce a main *r*-process pattern which is relatively similar to the observed solar abundances. The lowest entropy trajectory requires more neutron-rich initial conditions to produce nuclei up to the third solar *r*-process peak, with an initial electron fraction of $Y_{e,\,i} = 0.15$, compared to $Y_{e,\,i} = 0.25$ and $Y_{e,\,i} = 0.30$ for the $s/k = 100$ and 200 trajectories, respectively. In addition, while the temperature as a function of time looks the same for all three trajectories, the density is greater with lower entropy. Thus the equilibrium *r*-process path is farther from stability in the $s/k = 10$ case. As expected, we find significant variations in the nuclei with high F values. The clustering near closed shells at $Z = 50$, $N = 82$, and $N = 126$ persist but the location of the path and the extent to which photodissociation continues through freezeout influence exactly where the most impactful nuclei are found.

IV. CONCLUSION

Here we have presented a new binding energy sensitivity study for the *r* process and examined the impact of variations in astrophysical conditions on determining the list of most impactful nuclei. This paper is part of a series of sensitivity studies on the *r* process, which have included examinations of the sensitivity of the final *r*-process abundance pattern to individual neutron capture rates,[35,37–39] masses,[24,39] and β-decay rates.[39–41] Our next step is a complete nuclear mass sensitivity study where changes in the individual masses are carried through to all the nuclear parameters.[25] Our ultimate goal is tools to unravel the impact of nuclear data from the complications of the astrophysical scenario.

ACKNOWLEDGMENTS

This work was supported by the National Science Foundation under grant number PHY1068192 and through the Joint Institute for Nuclear Astrophysics grant number PHY0822648.

[1] C. Sneden, J. Cowan, and R. Gallino, Annu. Rev. Astro. Astrophys. **46**, 241 (2008).
[2] M. Arnould, S. Goriely, and K. Takahashi, Phys. Rep. **450**, 97 (2007).
[3] F.-K. Thielemann *et al.*, Prog. Part. Nucl. Phys. **66**, 346 (2011).
[4] K.-L. Kratz, J. Goerres, B. Pfeiffer, and M. Wiescher, Journal of Radioanalytical and Nuclear Chemistry **243**, 133 (2000).
[5] B. S. Meyer, G. J. Mathews, W. M. Howard, S. E. Woosley, and R. D. Hoffman, Astrophys. J. **399**, 656 (1992).
[6] S. E. Woosley, J. R. Wilson, G. J. Mathews, R. D. Hoffman, and B. S. Meyer, Astrophys. J. **433**, 229 (1994).
[7] A. Arcones, H.-Th. Janka, and L. Scheck, Astron. & Astrophys. **467**, 1227 (2007).
[8] L. Roberts, S. Reddy, and G. Shen, Phys. Rev. C **86**, 065803 (2012).
[9] C. Freiburghaus, S. Rosswog, and F.-K. Thielemann, Astrophys. J. **525**, L121 (1999).
[10] S. Goriely, A. Bauswein, and H.-Th. Janka, Astrophys. J. **738**, L32 (2011).
[11] O. Korobkin, S. Rosswog, A. Arcones, and C. Winteler, MNRAS **426**, 1940 (2012).
[12] R. Surman, G. McLaughlin, and W. Hix, Astrophys. J. **643**, 1057 (2006).
[13] S. Wanajo and H.-Th. Janka, Astrophys. J. **746**, 180 (2012).
[14] R. Surman, G. C. McLaughlin, M. Ruffert, H.-Th. Janka, and W. R. Hix, Astrophys. J. **679**, L117 (2008).
[15] S.-I. Fujimoto, K. Kotake, S. Yamada, M.-A. Hashimoto, and K. Sato, Astrophys. J. **644**, 1040 (2006).
[16] N. Nishimura *et al.*, Phys. Rev. C **85**, 048801 (2012).
[17] C. Winteler *et al.*, Astrophys. J. **750**, L22 (2012).
[18] P. Moller, J. R. Nix, W. D. Meyers, and W. J. Swiatecki, At. Data Nucl. Data Tables **59**, 185 (1995).
[19] G. Audi, F. G. Kondev, M. Wang, B. Pfeiffer, X. Sun, J. Blachot, and M. MacCormick, Chinese Physics C **36**, 1157 (2012).
[20] J. Duflo and A. Zuker, Phys. Rev. C **52**, R23 (1995).

[21] S. Goriely, N. Chamel, and J. Pearson, Phys. Rev. C **82**, 035804 (2010).
[22] N. Wang and M. Liu, Journal of Physics: Conference Series **420**, 012057 (2013).
[23] H. Schatz, Physics Today **61**(11), 40 (2008).
[24] S. Brett, I. Bentley, N. Paul, R. Surman, and A. Aprahamian, E. Phys. J. A **48**, 184 (2012).
[25] M. Mumpower *et al.*, in preparation.
[26] Y.-Z. Qian, P. Vogel, and G. J. Wasserburg, Astrophys. J. **494**, 285 (1998).
[27] Y.-Z. Qian and S. Woosley, Astrophys. J. **471**, 331 (1996).
[28] R. Surman and J. Engel, Phys. Rev. C **64**, 035801 (2001).
[29] T. Rauscher and F.-K. Thielemann, At. Data Nucl. Data Tables **75**, 1 (2000).
[30] S. Goriely, S. Hilaire, and A. J. Koning, Astron. Astrophys. **487**, 767 (2008).
[31] P. Moller, B. Pfeiffer, and K.-L. Kratz, Phys. Rev. C **67**, 055802 (2003).
[32] O. Tarasov and M. Hausmann, http://groups.nscl.msu.edu/frib/rates/fribrates.html (2012).
[33] B. S. Meyer, Phys. Rev. C **89**, 231101 (2002).
[34] M. Mumpower, G. C. McLaughlin, and R. Surman, Astrophys. J. **752**, 117 (2012).
[35] R. Surman, J. Beun, G. C. McLaughlin, and W. R. Hix, Phys. Rev. C **79**, 045809 (2009).
[36] M. R. Mumpower, G. C. McLaughlin, and R. Surman, Phys. Rev. C **85**, 045801 (2012).
[37] M. Mumpower, G. C. McLaughlin, and R. Surman, Phys. Rev. C **86**, 035803 (2012).
[38] R. Surman, M. Mumpower, R. Sinclair, K. L. Jones, W. R. Hix, and G. C. McLaughlin, AIP Advances **4**, 041008 (2014).
[39] R. Surman, M. Mumpower, J. Cass, I. Bentley, A. Aprahamian, and G. C. McLaughlin, *Proceedings of the International Nuclear Physics Conference (INPC)* (submitted) arXiv:1309.0059 (2013).
[40] J. Cass, G. Passucci, R. Surman, and A. Aprahamian, Proceedings of Science **NIC-XII 154** (2012).
[41] M. Mumpower, J. Cass, G. Passucci, R. Surman, and A. Aprahamian, AIP Advances **4**, 041009 (2014).